Materials Science and Engineering C 69 (2016) 46–51

Contents lists available at ScienceDirect

Materials Science and Engineering C

journal homepage: www.elsevier.com/locate/msec

Development of Co-based bulk metallic glasses as potential biomaterials

Zeyan Zhou [a], Qin Wei [b], Qiang Li [a,*], Bingliang Jiang [b,*], You Chen [b], Yanfei Sun [a]

[a] School of Physics Science and Technology, Xinjiang University, Urumqi, Xinjiang 830046, People's Republic of China
[b] First Affiliated Hospital of Xinjiang Medical University, Urumqi, Xinjiang 830046, People's Republic of China

ARTICLE INFO

Article history:
Received 14 March 2016
Received in revised form 8 April 2016
Accepted 5 May 2016
Available online 8 May 2016

Keywords:
Co-based bulk metallic glasses
Biomaterials
Corrosion resistance
Biocompatibility

ABSTRACT

A new series of $Co_{80-x-y}Cr_xMo_yP_{14}B_6$ (x = 5 y = 5; x = 5 y = 10; x = 10 y = 10, all values in at.%) bulk metallic glasses (BMGs) with a maximum diameter of 1.5 mm has been developed for using them as potential bio-implant materials by a combination of fluxing treatment and J-quenching technique. The performance of the present Co-based BMGs in biomedical implant applications was investigated as compared to the CoCrMo biomedical alloy (ASTM F75) and 316L stainless steel (316L SS). The corrosion behavior of the samples was investigated in both Hank's solution (pH = 7.4) and artificial saliva solution (pH = 6.3) at 37 °C employing electrochemical measurements. The results indicate that the Co-based BMGs exhibit much higher corrosion resistance in the simulated body solutions than that of 316L SS. Compared with the corrosion resistance of ASTM F75, that of $Co_{70}Cr_5Mo_5P_{14}B_6$ and $Co_{65}Cr_5Mo_{10}P_{14}B_6$ BMGs is found to be lower and that of $Co_{60}Cr_{10}Mo_{10}P_{14}B_6$ BMG is higher. The concentrations of Co, Cr, and Mo ions released into the simulated body solutions from our Co-based BMGs after potentiodynamic polarization are significantly lower than that released from ASTM F75. The biocompatibility of the specimens was evaluated using an *in vitro* test of NIH3T3 cell culture in the specimen extraction media for 1, 3, 5, and 7 days, revealing the non-cytotoxicity of the Co-based BMGs towards NIH3T3 cells. Moreover, examinations on the cell adhesion and growth on the surface of the specimens indicate that the Co-based BMGs exhibit better cell viability compared to ASTM F75 and 316L SS biomedical alloys.

1. Introduction

Metallic biomaterials have the longest history among various biomaterials, and they have been extensively used in different parts of the human body such as in artificial valves in the heart, stents in blood vessels, and replacement implants in shoulders, knees, hips, elbows, ears, and orodental structures [1–3]. Despite the large number of metals and alloys produced in the industry, the specific requirements such as the corrosion resistance and the biocompatibility restrict the use of available commercial metallic materials as biomaterials. The commercial metallic biomaterials can be classified into the following four groups: stainless steels, Co-based alloys, Ti-based alloys, and other miscellaneous materials (*e.g.* NiTi shape memory alloy and alloys of Mg and Ta) [4]. Among these metallic biomaterials, Co-based alloys exhibit good biocompatibility, excellent mechanical properties, and a high corrosion resistance. Hence, they have been widely used as artificial joints in biomedical implants [5–6]. However, the use of Co-based alloy implants is limited owing to their degradation due to the corrosion environment in the body, which reduces their long-term stability and leads to releasing of toxic ions and wear particles into the body [7]. Therefore, further improvements in the corrosion and wear resistance and mechanical properties of the Co-based alloy biomaterials are crucial for their applications in biomedical implants.

With the development of novel biomedicine materials, bulk metallic glasses (BMGs) have attracted significant attention owing to their several desired properties in biomedical implant applications, including excellent biocompatibility, corrosion resistance and wear resistance, high strength, low Young's modulus, and simple processing capabilities compared to the crystal alloy counterparts [8]. Thus, Ti- [9–11], Zr- [12–14] and Fe-based [15–17] BMGs have been developed for biomedical implant applications during the past two decades, and they exhibit enhanced performances as biomedical implant biomaterials compared to several conventional metallic biomaterials. Co-based alloys constitute an important member in the family of metallic biomaterials; however, the applications of Co-based BMGs as biomaterials implants have not yet been investigated.

In this work, a new series of $Co_{80-x-y}Cr_xMo_yP_{14}B_6$ (x = 5 y = 5; x = 5 y = 10; x = 10 y = 10, all values in at.%) BMGs is developed for biomedical implant applications by means of a combination of fluxing treatment and J-quenching techniques [18]. The corrosion performance, ionic releasing, and the biocompatibility of the Co-based BMGs are investigated and compared with those of CoCrMo biomedical alloys (ASTM F75) and 316L stainless steel (316L SS).

* Corresponding authors.
E-mail addresses: qli@xju.edu.cn (Q. Li), gaohan410@126.com (B. Jiang).

http://dx.doi.org/10.1016/j.msec.2016.05.025
0928-4931/

2. Materials and methods

2.1. Material preparation and characterization

$Co_{80-x-y}Cr_xMo_yP_{14}B_6$ (x = 5 y = 5; x = 5 y = 10; x = 10 y = 10, all values in at.%) master alloy ingots were prepared by torch-melting a mixture of high-pure Co powder (99.9 mass%), Cr powder (99.9 mass%), Mo powder (99.9 mass%), Co_2P powder (99.9 mass%), and B piece (99.9 mass%) under high-purity argon atmosphere. The master alloy ingots were then fluxed in a fluxing agent composed of B_2O_3 and CaO with a mass ratio of 3:1 at a temperature of about 1500 K for 4–5 h under vacuum corresponding to a residual pressure of ~50 Pa. After fluxing, the specimens were cooled down to ambient temperature followed by subjecting them to J-quenching, the details of which can be found elsewhere [19] to obtain alloy rods with a diameter of 1.0 mm and length of several centimeters. The glassy nature of the as-cast specimens was examined using X-ray diffraction (XRD, Bruker D2 PHASER) with Cu Kα radiation (30 kV and 30 mA) at room temperature. The thermal behavior of the as-cast specimens was examined by differential scanning calorimetry (DSC, NETZSCH DSC 404C F1) with a heating rate of 0.33 K/s under Ar atmosphere.

2.2. Electrochemical measurements

Electrochemical measurements of the specimens of Co-based BMGs, 316L stainless steel (316L SS), and CoCrMo biomedical alloy (ASTM F75, purchased from Jinyehongtai Metals Co. Ltd., Beijing, China), were examined using a CS315 electrochemical workstation. Electrochemical polarization was carried out in a three-electrode cell using a platinum auxiliary electrode, a saturated calomel reference electrode, and a test specimen as the working electrode in 200 mL electrolytes in air. The whole cell was maintained at 37 °C throughout the test. Hank's solution (pH 7.4) and artificial saliva solution (pH 6.3) were used as electrolytes in the present study, which were purchased from Biohao Biotechnology Co. Ltd. (Beijing, China). Prior to the test, the work surface of the specimens was mechanically polished with 2400-grit wet sand paper washed with distilled water, and dried in air. Potentiodynamic polarization curves of the specimens were recorded from − 1.0 V to 1.5 V with a scan rate of 0.2 mV/s after immersing the specimens in electrolytes for 1 h for obtaining a steady open-circuit potential. The corrosion parameters, namely, the corrosion potential (E_{corr}), corrosion current density (I_{corr}), pitting potential (E_{pit}), and corrosion rate (CR) were determined from the potentiodynamic polarization curves to evaluate the corrosion resistance of the specimens.

2.3. Scanning electron microscopy (SEM) observations

The surface morphology of the specimens after cell adhesion was examined by SEM at 5 kV in secondary electron mode.

2.4. Inductively coupled plasma atomic emission spectrometry (ICP-AES) measurements

A full spectrum direct reading ICP-AES was employed to measure the concentrations of ions dissolved from the specimens into the Hank's solution and artificial saliva solution after potentiodynamic polarization. An average of three measurements was taken for each sample.

2.5. Cell culture

Mouse embryonic fibroblast cell (NIH3T3 cell) lines were cultured in 10 mL RPMI 1640 medium (purchased from GIBCO laboratories, Grand Island, NY USA) with 10% fetal bovine serum (FBS), 100 U/mL penicillin, and 100 μg/mL streptomycin at 37 °C in a humid atmosphere of 5% CO_2. Cells were washed and incubated in a fresh medium for 24 h followed by changing to a new medium. After 72 h, the bottle was full of cells. Subsequently, 0.25% trypsin solution was added to shed the cells followed by the addition of a growth medium (90 mL 1640 + 10 mL FBS + 100 μL P/S) to stop the reaction. Cells were counted as needed.

2.6. Cytotoxicity test

The Co-based BMGs and 316L SS rods with a diameter of 1 mm and ASTM F75 square bar with a cross-sectional area of 2 mm × 2 mm were cut into thin wafers of 0.8 mm thickness. One side of the wafers was polished to a mirror finish using 2400-grit wet sand paper until the final thickness of the wafers was around 0.5 mm. The wafers were washed successively with acetone, absolute ethyl alcohol, and deionized water by ultrasonication for 20 min and were dried in air. The wafers were packed and sterilized in a high-pressure steam sterilization pot. Five samples of each specimen were plated with the mirror side up to obtain each of three 96-well cell culture plates, and the experiments were performed on a super clean bench in a bioclean room. Cells were incubated in 96-well cell culture plates with 2500 cells per well. After incubating the cells in a humid atmosphere with 5% CO_2 at 37 °C for 1, 3, 5, and 7 days, 10 μL of Cell Counting Kit-8 (CCK-8) was added to each well avoiding blister followed by further incubation with CCK-8 at 37 °C for 1.5 h. The samples were then collected for spectrophotometrical absorbance measurements using a microplate reader at 450 nm.

Four replicates (both the samples and controls) were used for all tests. The cell viability ratio (R_{cv}) of each sample was calculated using the equation: R_{cv} = (cell viability in experimental extract)/(cell viability in negative control).

2.7. Cell adhesion

The Co-based BMGs with a diameter of 1 mm, 316L SS rods with a diameter of 1 mm, and ASTM F75 square bar with a cross-sectional area of 2 mm × 2 mm were used for the cell adhesion test. The test specimens were prepared in the same way as in the cytotoxicity test. 1 mL cell suspension was seeded onto the polished side of the wafers with a cell density of 2500 cells per well in 24-well plates. After 5 days of culture in a humid atmosphere with 5% CO_2 at 37 °C, the cell-seeded discs were washed with D-Hank's three times before fixing with 3% glutaraldehyde for 1.5 h and dehydrated using tertiary butanol and absolute ethyl alcohol in proportions of 30%, 50%, 70%, 80% and 90% for 10 min each time at room temperature (25 °C), respectively. After rinsing twice with 100% tertiary butanol, the 24-well plates were placed in fridge at a temperature below 4 °C for 30 min followed by placing in a vacuum coater machine to remove the frost and vacuum coating in order to analyze the surface morphology of the cells using SEM.

3. Results and discussion

3.1. XRD analysis and GFA

Fig. 1 shows XRD patterns of the as-cast $Co_{80-x-y}Cr_xMo_yP_{14}B_6$ (x = 5 y = 5; x = 5 y = 10; x = 10 y = 10, all values in at.%) glassy alloy rods of the maximum diameter (D_{max}). The XRD patterns exhibit broad diffuse peaks at a diffraction angle (2θ) of about 43°, and Bragg peaks corresponding to crystalline phases are not observed, indicating the fully glassy nature of the specimens. As $Co_{80-x-y}Cr_xMo_yP_{14}B_6$ BMGs do not contain any harmful elements (such as Ni, Al, Cu, *etc.*) and rare earth elements, they could be used as potential biomedical implant materials. The diameter of the specimens used in the subsequent tests is 1.0 mm, which is less than D_{max} of the Co-based alloys, in order to avoid partial crystallization. For convenience, $Co_{70}Cr_5Mo_5P_{14}B_6$, $Co_{65}Cr_5Mo_{10}P_{14}B_6$, and $Co_{60}Cr_{10}Mo_{10}P_{14}B_6$ BMGs are hereafter denoted as Cr_5Mo_5, Cr_5Mo_{10}, and $Cr_{10}Mo_{10}$, respectively.

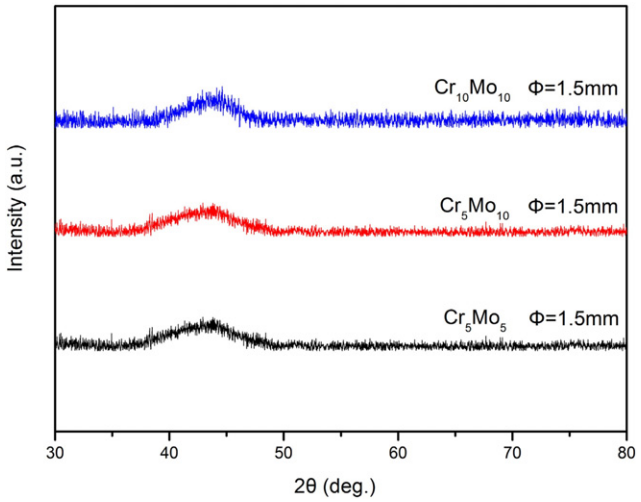

Fig. 1. XRD patterns of the Co-based BMGs with the maximum diameter for complete glass formation (D_{max}).

Fig. 2 shows DSC thermal scans of the Co-based glassy alloy specimens recorded with a heating rate of 0.33 K/s. Fig. 2 reveals that all the specimens exhibit a clear glass transition followed by an extended supercooled liquid region and a single or multi-stage crystallization process. The glass transition temperature (T_g), onset crystallization temperature (T_x), melting temperature (T_m), and the liquidus temperature (T_l) obtained from the DSC curves (marked by arrows in Fig. 2) are summarized in Table 1. The Co-based BMGs exhibit a relatively high T_g of ~760 K and a large supercooled liquid region ($\Delta T_x = T_x - T_g$) of ~40 K, indicating a high thermal stability.

3.2. Electrochemical measurements

Fig. 3 shows potentiodynamic polarization curves of the Co-based BMGs, 316L SS, and ASTM F75 in air at 37 °C in both Hank's solution and artificial saliva solution after solidification encapsulated with epoxy resin glue. The corrosion potential (E_{corr}), pitting potential (E_{pit}), corrosion current density (I_{corr}), and the pitting current density (I_{pit}) determined from potentiodynamic polarization curves and the corrosion rate (CR) derived from I_{corr} are summarized in Table 2. All the samples exhibit a stable passivation region in the polarization curve as shown in Fig. 3. Compared with 316L SS and ASTM F75, our Co-based BMGs,

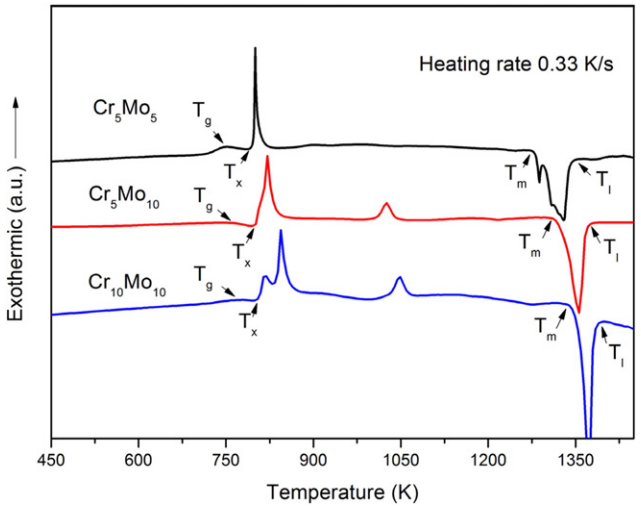

Fig. 2. DSC thermal scans of the Co-based BMGs recorded with a heating rate of 0.33 K/s.

Table 1
Critical diameter for complete glass formation (D_{max}) and the thermal parameters (T_g: glass transition temperature, T_x: onset temperature of crystallization, T_m: melting temperature, T_l: liquidus temperature) of Cr_5Mo_5, Cr_5Mo_{10}, and $Cr_{10}Mo_{10}$ bulk glassy rod alloys determined from the DSC curves recorded with a heating rate of 0.33 K/s.

Specimens	D_{max} (mm)	T_g (K)	T_x (K)	T_m (K)	T_l (K)
Cr_5Mo_5	1.0	757	797	1267	1348
Cr_5Mo_{10}	1.0	758	799	1308	1385
$Cr_{10}Mo_{10}$	1.0	762	803	1355	1397

especially $Cr_{10}Mo_{10}$, exhibit a higher E_{pit} and a wider passivation region ($\Delta E_{pit} = E_{pit} - E_{corr}$), indicating a higher pitting corrosion resistance. Co-based BMGs exhibit a very low I_{corr} of the order of 10^{-7} A·cm^{-2} and a low CR of the order of 10^{-3} mm·year^{-1} in both Hank's solution and artificial saliva solution, indicating excellent corrosion resistance of the samples. The I_{corr} and CR values of the Co-based BMGs decrease with increase in the Cr and Mo contents. Cr and Mo are known to be corrosion resistance elements, which can form a more stable passive film than that of Co during the corrosion process [20–21]. Therefore, the corrosion resistance of the Co-based BMGs is enhanced with increase in the Cr and Mo contents. The I_{corr} and CR values of the Co-based BMGs are much lower than those of 316L SS. Compared with those of ASTM F75, the I_{corr} and CR values of Cr_5Mo_5 and Cr_5Mo_{10} are higher, but those of $Cr_{10}Mo_{10}$ are lower. ASTM F75 contains a much higher Cr content (~28 at.%) than that of the Co-based BMGs, which could be attributed

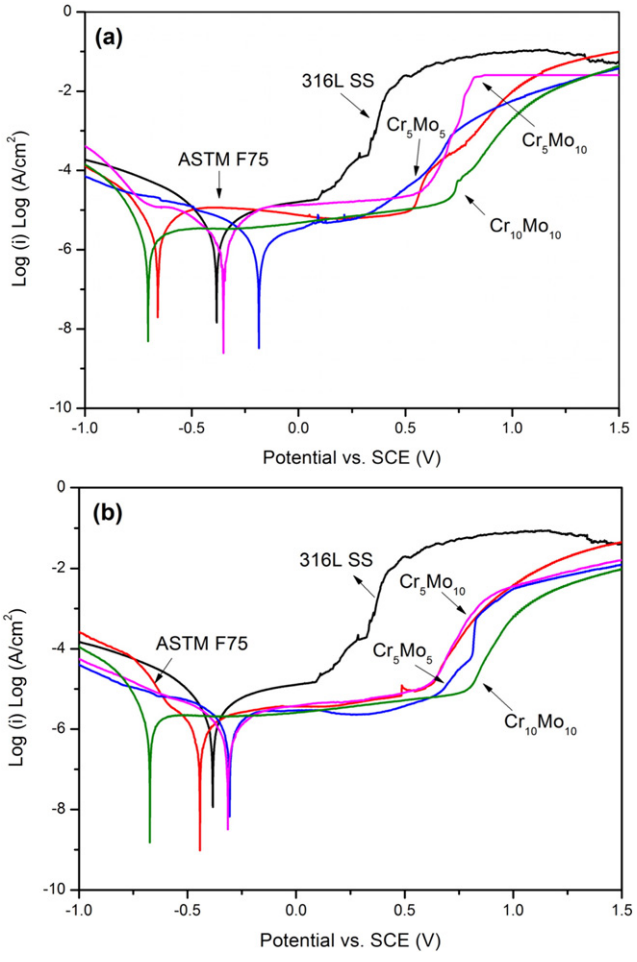

Fig. 3. Potentiodynamic polarization curves in (a) Hank's solution and (b) artificial saliva solution of the Co-based BMGs, 316L SS, and ASTM F75 in air at 37 °C.

Table 2
Results obtained by potentiodynamic polarization in air at 37 °C. I_{corr}: corrosion current density; E_{corr}: corrosion potential; E_{pit}: pitting potential; ΔE_{pit}: passivation region defined as $E_{pit} - E_{corr}$; *CR*: corrosion rate derived from I_{corr}.

Alloy	Solution	I_{corr}	E_{corr}	E_{pit}	ΔE_{pit}	CR
		(10^{-7} A·cm^{-2})	(mV)	(mV)	(mV)	(10^{-3} mm·year^{-1})
316L SS	Hanks's	13.84	−373	122	476	10.91
	Saliva	12.58	−383	132	515	9.99
ASTM F75	Hanks's	7.68	−660	480	1340	6.10
	Saliva	4.17	−446	485	931	3.32
Cr_5Mo_5	Hanks's	8.51	−185	301	486	6.76
	Saliva	7.90	−317	626	943	6.28
Cr_5Mo_{10}	Hanks's	8.83	−347	574	921	7.01
	Saliva	6.74	−313	630	943	5.35
$Cr_{10}Mo_{10}$	Hanks's	7.00	−707	694	1401	5.56
	Saliva	3.31	−671	788	1459	2.63

to the high corrosion resistance of ASTM F75. However, the corrosion resistance of $Cr_{10}Mo_{10}$ is superior to ASTM F75, which could be contributed to the structurally and chemically homogenous amorphous structure of the BMGs, which results in the formation of a uniform and stable surface passive film, thereby protecting the alloy against corrosion [22]. In addition, the corrosion resistance of the Co-based BMGs in artificial saliva solution is better than that in Hank's solution as can be seen from Table 2 and Fig. 3, making the Co-based BMGs suitable for dental implant applications [23].

3.3. Metal ion release

Fig. 4 shows the concentrations of ions dissolved in the Hank's solution and the artificial saliva solution from the Co-based BMGs, 316L SS, and ASTM F75 after potentiodynamic polarization. The metal ions released from 316L SS in both the simulated body solutions include Fe, Ni, Mn, Cr, and Mo ions, and those released from ASTM 75 and Co-based BMGs are mostly Co, Cr, and Mo ions. Compared with ASTM F75, the Co-based BMGs release smaller amounts of Co and Cr ions, which could be ascribed to their lower Co and Cr contents and higher corrosion resistance. Additionally, the amounts of released Co and Cr ions for different samples are in the order $Cr_5Mo_5 > Cr_5Mo_{10} > Cr_{10}Mo_{10}$, in accordance with the order of corrosion resistance of the three alloys.

The concentration of ions released from the Co-based BMGs and ASTM F75 is very low, which could be attributed to the high corrosion resistance of the alloys. Especially, Co-based BMGs have a lower Co ion content than that of ASTM F75. Considering human health concerns, the implant materials should have a low content of toxic ions such as Co, Cr, and Mo ions. Therefore, Co-based BMGs are found to be a better candidate than ASTM F75 in biomedical applications.

3.4. Biocompatibility

Fig. 5 presents the cytotoxicity of NIH3T3 cells using the Co-based BMGs, 316L SS, and ASTM F75 extraction media for 1, 3, 5, and 7 days. Co-based BMGs exhibit the highest cell viability among all the specimens and 316L SS exhibits the lowest. Furthermore, the cell viability of Co-based BMGs is higher than that of the negative control carried out for 1 to 7 days, indicating that almost no cytotoxicity is observed with the Co-based BMGs on NIH3T3 cells. As specimens are immersed in the cell suspension, harmful metal ions such as Co, Cr, Ni, and Fe ions could be released to the cells. Among these metal ions, Co, Ni, and Cr ions have high cytotoxic effects on the cells [24]. From the metal ion release test, the Co-based BMGs are known to release small amounts of Co and Cr ions (and no Ni ions), thereby exhibiting the highest cell viability among the three alloys.

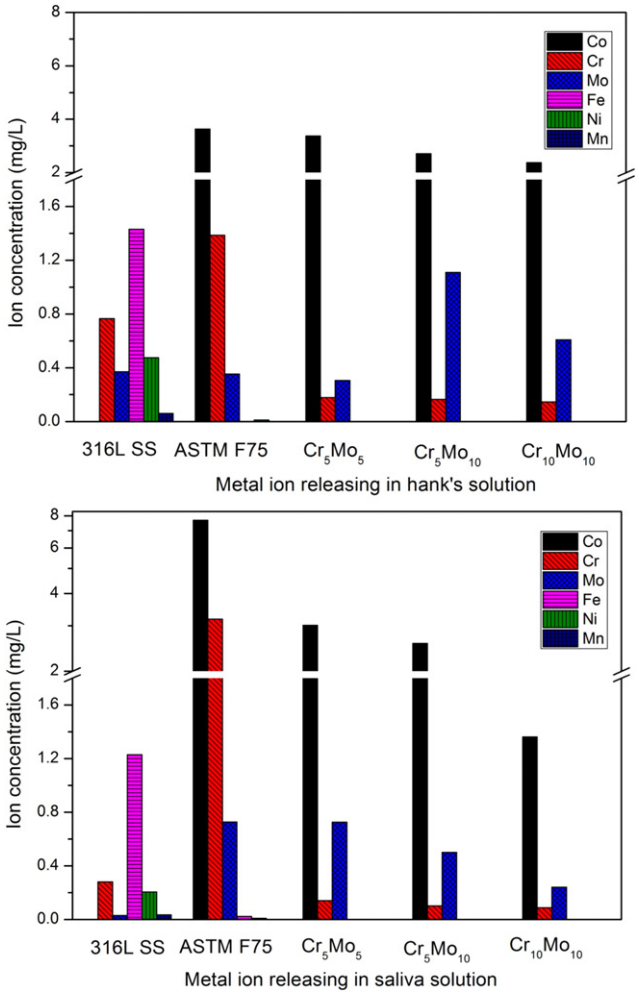

Fig. 4. Concentrations of ions dissolved in the Hank's solution and the artificial saliva solution after potentiodynamic polarization.

Fig. 6 presents SEM images, recorded under different magnifications, of the NIH3T3 cells cultured on the specimens for 5 days. The surfaces of the samples are covered with a thick layer of NIH3T3 cells. However, the coverage of NIH3T3 cells on the surface of 316L SS is lesser compared to

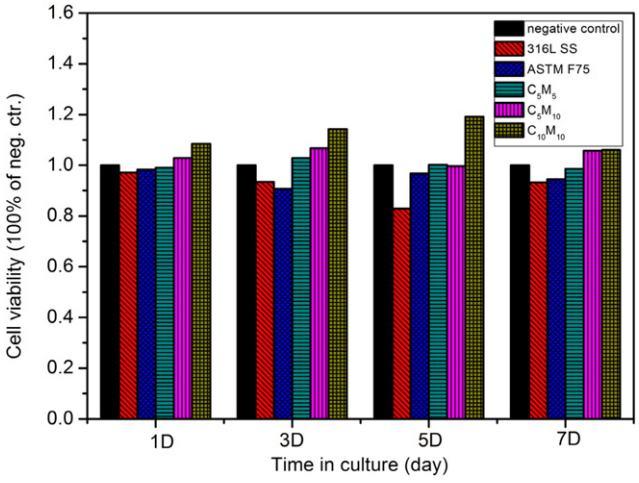

Fig. 5. Cytotoxicity of NIH3T3 cells in the Co-based BMGs, 316L SS, and ASTM F75 extraction media for 1, 3, 5, and 7 days.

that of ASTM F75 and the Co-based BMGs. Furthermore, the cells on the surface of 316L SS are found to be exhibit a flat morphology (not plump). The poor biocompatibility of 316L SS could be attributed to the considerable amounts of Ni ions released, which have a higher cytotoxic effect on the NIH3T3 cells compared to other ions. Cells adherent on the ASTM F75 and the Co-based BMGs exhibit a plump morphology, indicating enhanced cell growth conditions. However, several small white bulbs can be observed on the surface of ASTM F75, which might correspond to dead cells. These small bulbs are rarely observed on the surface of the Co-based BMGs. Compared to the Co-based BMGs, ASTM F75 releases higher amounts of toxic Co ion, which could be attributed to the higher number of dead cells on the sample. Considering different Co-based BMGs, the cells on the surface of $Cr_{10}Mo_{10}$ exhibit a more distinct plump morphology owing to the best cell adhesion

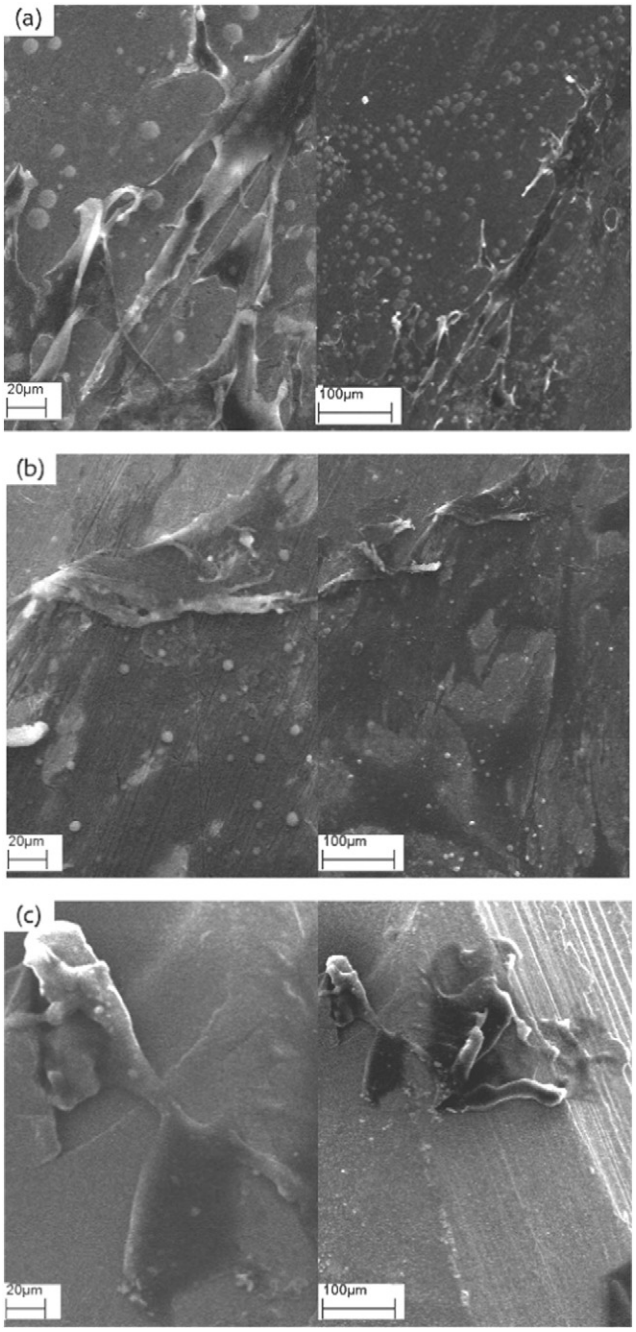

Fig. 6. SEM images of NIH3T3 cells cultured on 316L SS (a), ASTM F75 (b), Cr_5Mo_5 (c), Cr_5Mo_{10} (d), and $Cr_{10}Mo_{10}$ (e) for 5 days. Left part of the figure shows high magnification images.

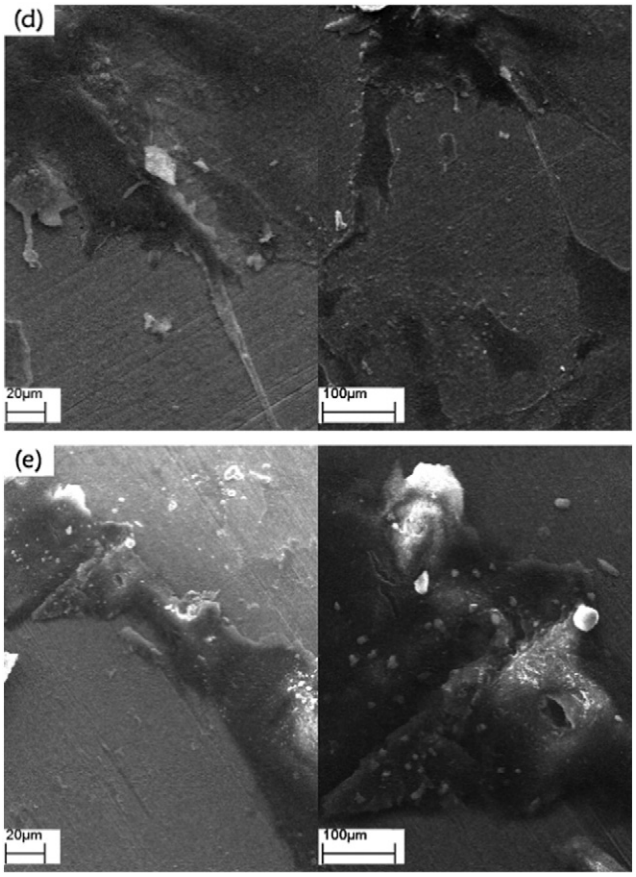

Fig. 6 (*continued*).

compared to other samples. The NIH3T3 cell adhesion and the cytotoxicity tests with NIH3T3 cells indicate that the Co-based BMGs, especially $Cr_{10}Mo_{10}$, exhibit a higher biocompatibility compared with that of ASTM F75 and 316L SS.

4. Conclusions

In this work, a new series of $Co_{80-x-y}Cr_xMo_yP_{14}B_6$ ($x = 5, y = 5$; $x = 5, y = 10$; $x = 10, y = 10$, all values in at.%) BMGs with a maximum diameter of 1.5 mm have been successfully prepared by combining fluxing treatment and J-quenching techniques. Co-based BMGs exhibited much higher corrosion resistance than that of 316L SS. Compared with the corrosion resistance of ASTM F75, Cr_5Mo_5 and Cr_5Mo_{10} exhibited lower corrosion resistance and $Cr_{10}Mo_{10}$ exhibited higher. Compared with 316L SS and ASTM 75, the Co-based BMGs release a smaller amount of harmful ions, thereby exhibiting a higher cell viability in the Hank's solution and the artificial saliva solution. Morphological analysis after the cell adhesion test indicated that NIH3T3 cells with a plump morphology are well grown on the surface of the Co-based BMGs, indicating the non-cytotoxicity and the good biocompatibility of the Co-based BMGs. Our results suggest that the Co-based BMGs could be a better candidate for biomedical implant applications than ASTM F75. Among the prepared Co-based BMGs, $Cr_{10}Mo_{10}$ exhibits the highest corrosion resistance and biocompatibility, making it the most suitable for biomedical implant applications.

Acknowledgements

This research was sponsored by the National Natural Science Foundation of China (Grant No. 51261028 and 51561028).

References

[1] S. Ramakrishna, J. Mayer, E. Wintermantel, K.W. Leong, Biomedical applications of polymer-composite materials: a review, Compos. Sci. Technol. 61 (2001) 1189–1224.
[2] D.L. Wise, Biomaterials Engineering and Devices, Humana Press, Berlin, 2000 205–319.
[3] J.B. Park, J.D. Bronzino (Eds.), Biomaterials: Principles and Applications, CRC Press, Boca Raton, FL 2003, pp. 1–241.
[4] D.J. Blackwood, Corros. Rev. 21 (2003) 97–124.
[5] Metals Handbook, Corrosion, ninth ed.Vol. 13 ASM International, 1987.
[6] D.F. Williams, The properties and clinical uses of cobalt–chromium alloys, Biocompatibility of Clinical Implant Materials, CRC Press, Inc., Boca Raton, Florida, vol. 1, 1981.
[7] S. Mischler, A. Igual Munoz, Wear of CoCrMo alloys used in metal-on-metal hip joints: a tribocorrosion appraisal, Wear 297 (2013) 1081–1094.
[8] J. Schroers, G. Kumar, T.M. Hodges, S. Chan, T.R. Kyriakides, Bulk metallic glasses for biomedical applications, JOM 61 (2009) 21–29.
[9] M. Calin, et al., Designing biocompatible Ti-based metallic glasses for implant applications, Mater. Sci. Eng. C 33 (2013) 875–883.
[10] A. Blanquer, E. Pellicer, A. Hynowska, L. Barrios, E. Ibáñez, M.D. Baró, J. Sort, C. Nogués, In vitro biocompatibility assessment of Ti40Cu38Zr10Pd12 bulk metallic glass, J. Mater. Sci. 25 (2014) 163–172.
[11] F. Qin, M. Yoshimura, X. Wang, S. Zhu, A. Kawashima, K. Asami, A. Inoue, Corrosion behavior of a Ti-based bulk metallic glass and its crystalline alloys, Mater. Trans. 48 (2007) 1855–1858.
[12] G. Xie, W. Zhang, D.V. Louzguine-Luzgin, H. Kimura, A. Inoue, Fabrication of porous ZrCuAlNi bulk metallic glass by spark plasma sintering process, Scr. Mater. 55 (2006) 687–690.
[13] G. Xie, D.V. Louzguine-Luzgin, H. Kimura, A. Inoue, Fabrication of ZrCuAlNi metallic glassy matrix composite containing ZrO2 particles by spark plasma sintering process, Mater. Trans. JIM 48 (2007) 158–162.
[14] G. Xie, D.V. Louzguine-Luzgin, F. Wakai, H. Kimura, A. Inoue, Microstructure and properties of ceramic particulate reinforced metallic glassy matrix composites fabricated by spark plasma sintering, Mater. Sci. Eng. B 148 (2008) 77–81.
[15] S. Li, Q. Wei, Q. Li, B. Jiang, Y. Chen, Y. Sun, Development of Fe-based bulk metallic glasses as potential biomaterials, Mater. Sci. Eng. C 52 (2015) 235–241.
[16] Y. Wang, H. Li, Y. Cheng, S. Wei, Y. Zheng, Corrosion performances of a nickel-free Fe-based bulk metallic glass in simulated body fluids, Electrochem. Commun. 11 (2009) 2187–2190.
[17] Y. Wang, H. Li, Y. Zheng, M. Li, Corrosion performances in simulated body fluids and cytotoxicity evaluation of Fe-based bulk metallic glasses, Mater. Sci. Eng. C 32 (2012) 599–606.
[18] Q. Li, J. Li, P. Gong, K. Yao, J. Gao, H. Li, Formation of bulk magnetic ternary Fe80P13C7 glassy alloy, Intermetallics 26 (2012) 62–65.
[19] Q. Li, Formation of ferromagnetic bulk amorphous Fe40Ni40P14B6 alloys, Mater. Lett. 60 (2006) 3113–3117.
[20] M.W. Tan, E. Akiyama, H. Habazaki, A. Kawashima, K. Asami, K. Hashimoto, The role of chromium and molybdenum in passivation of amorphous Fe-Cr-Mo-P-C alloys in deaerated 1 M HCl, Corros. Sci. 38 (1996) 2137–2151.
[21] M. Naka, K. Hashimoto, T. Masumoto, Effect of addition of chromium and molybdenum on the corrosion behavior of amorphous Fe-20B, Co-20B and Ni-20B alloys, J. Non-Cryst. Solids 34 (1979) 257–266.
[22] C. Suryanarayana, A. Inoue, Bulk Metallic Glasses, Taylor and Francis, 2010 P307.
[23] H. Zohdi, H.R. Shahverdi, S.M.M. Hadavi, Effect of Nb addition on corrosion behavior of Fe-based metallic glasses in Ringer's solution for biomedical applications, Electrochem. Commun. 13 (2011) 840–843.
[24] M. Niinomi, Metals for Biomedical Devices, CRC Press, Cambridge, UK, 2010.